Normal Colon

Thomas Mang, Gernot Böhm, and Wolfgang Schima

Contents

T. Mang, M.D. (✉)
Department of Radiology, Medical University of Vienna, Waehringer Guertel 18-20, 1090 Vienna, Austria
e-mail: thomas.mang@meduniwien.ac.at

G. Böhm, M.D.
Abteilung für Diagnostische und Interventionelle Radiologie, A.ö. Krankenhaus der Elisabethinen Linz, Fadingerstrasse 1, 4010 Linz, Österreich, Austria

W. Schima, M.D., M.Sc.
Abteilung für Diagnostische und Interventionelle Radiologie, KH Göttlicher Heiland, KH der Barmherzigen Schwestern Wien und Sankt Josef KH, Dornbacher Strasse 20-28, 1170 Vienna, Austria

Abstract

Aim of this chapter is to describe the normal anatomy of the colon on the basis of 2D and 3D CT colonography criteria.

In normal colon the wall thickness is thin (less than 2 mm) and may increase to 5 mm in collapsed segments.

The colon is generally recognized by three morphologic key features, which can be clearly identified in CT colonography: the semilunar folds, the taeniae, and the haustra.

The normal colon typically is divided in antegrade order into six segments: the cecum with the ileocecal valve and the appendix, the ascending colon, the transverse colon, the descending colon, the sigmoid colon, and the rectum. The splenic and the hepatic flexure should not be considered separate segments.

The ileocecal valve has a variable appearance, being classified as either labial, when it appears as a slit-like opening; papillary, when its shape is dome-like; or intermediate.

Cases showing the normal colon anatomy are presented in the chapter.

Introduction

A fundamental prerequisite for radiologists aiming to read CT colonographic examinations is a thorough knowledge of the normal anatomy of the colon. Although the large bowel has been examined by radiologists for decades with barium studies, a CT colonographic evaluation may provide a different view of the colon [1–3]. Indeed, CT colonography is quite accurate for assessing the anatomy of the colon. However, the planar 2D approach to trace the gas-distended colon may result in new challenges for some readers, since the complex intraluminal anatomy of bowel loops and haustral folds may complicate the evaluation [4]. Moreover, some radiologists may not be familiar with the "intraluminal" perspective provided by an endoluminal 3D evaluation. Thus, a combined two-dimensional and three-dimensional imaging approach is considered the best practice for

E. Neri et al. (eds.), *CT Colonography Atlas,* Medical Radiology,
DOI 10.1007/978-3-642-11149-5_1,

CT colonographic evaluation [5]. In this chapter the normal anatomy of the colon is described on the basis of 2D and 3D CT colonographic imaging criteria.

CT Colonography Morphology

General Two-Dimensional and Three-Dimensional CT Features of the Colonic Wall

Wall Thickness

In CT colonographic examinations, after colonic gas insufflation, the wall of the distended normal colon is very thin, measuring less than 2 mm [6]. Typically, it should be barely perceptible on 2D CT colonographic images and may be better depicted with abdominal window settings. In collapsed colonic segments, the colonic wall thickness increases physiologically to up to 5 mm or, in case of spasms, up to 8 mm (Fig. 1) [6]. The normal colonic wall itself has soft tissue attenuation on 2D CT colonographic images. It may show a slight enhancement after intravenous contrast media application. The colon is surrounded by fat tissue, which shows a homogeneous hypodense structure. On endoluminal 3D images, the normal colon presents with a smooth surface.

Morphologic Key Features of the Colon Wall

The colon is generally recognized by three morphologic key features, which can be identified on CT colonographic images: the semilunar folds, the taeniae, and the haustra (Fig. 1) [7].

The semilunar folds (plicae semilunares) are thin crescent-shaped structures. They are oriented orthogonally to the course of the colon and are located one after another in a row when passing through the coloni. Typically, the three rows of colonic folds are each separated by a taenia (see below).

On 2D CT colonographic images, normal semilunar folds are typically very thin and regular soft tissue structures. They are better recognized with wide window settings. On 3D endoluminal views, these folds are seen as crescent-shaped thin folds with a smooth surface. They can be thickened in regions of suboptimal colonic distention or form complex structures, especially at the inner parts of the flexures. The size and number of semicircular folds may vary individually and also within a single patient, due to the peristaltic activity of the colon.

The *taeniae* (taeniae coli) are three longitudinal muscular bands, which are formed from the longitudinal muscle layer of the colonic wall, each with a width of approximately 8 mm. They run along the length of the colon and are located on the anterior, dorsolateral, and dorsomedial wall section [8]. The three taeniae are most prominent in the transverse and ascending colon and, finally, coalesce at the cecum in the area of the appendiceal orifice. The taeniae are less prominent toward the descending and the sigmoid colon and disappear at the rectosigmoid junction.

Haustra are saccular outpouchings of the colonic wall, which are located in the spaces between the taeniae. The haustra are separated by the semilunar folds along the course of the colon. Haustra may vary in prominence due to the contraction of the taeniae and the peristaltic activity of the colon.

Segments of the Colon

The normal colon typically frames the abdomen. It is divided in antegrade order into six segments: the cecum with the ileocecal valve and the appendix, the ascending colon, the transverse colon, the descending colon, the sigmoid colon, and the rectum (Fig. 3). The splenic and the hepatic flexure are not considered separate segments [9].

The length and the diameter of the colon have been evaluated with CT colonography by Khasab et al. [10]. The mean total colonic length, evaluated in this study, was 189.5 cm with a range of 120–299 cm, with the transverse and sigmoid colon representing the longest and the cecum and rectum the shortest segments. The transverse diameter of the colon varied greatly. The cecum has the widest luminal diameter (7.6 cm), followed by the rectum (6.5 cm) and the ascending colon (6.1 cm). The sigmoid (3.5 cm) and descending colon (3.8 cm) have the narrowest luminal diameter [10]. Variations in the segmental or total length of the colon, as well as the length in the segmental location, are not uncommon. Some of these variations are clinically relevant. They are described in Chap. 2 (page 17, Rosa Bouzas).

The cecum is the first segment of the colon (Fig. 4). It is typically located in the right iliac fossa and represents a blind sac. At its base, the colonic taeniae converge and form the triradiate fold. Here, the appendiceal orifice can be seen on endoluminal 3D images as a small, well-circumscribed, round or oval depression of the colonic wall [1].

The *ileocecal valve* anatomically separates the cecum from the ascending colon (Fig. 5). It is located at the junction of the terminal ileum and the colon. The ileocecal valve is most commonly located on the medial side of the cecum, although anatomic variants exist. On 3D endoluminal images, the valve is typically shown with an upper lip and a lower lip [11]. The ileocecal valve has a variable appearance, being classified as either labial, when it appears as a slit-like opening, papillary, when its shape is dome-like, or intermediate. The orifice of the ileocecal valve can be seen as a tiny central depression [12]. Two-dimensional CT images demonstrate the connection of the terminal ileum to the valve. The ileocecal valve may have a wide range of attenuation values, with heterogeneous attenuation. It commonly contains fat tissue and is then referred to as a lipomatous ileocecal valve [13].

The *ascending colon* extends into the right abdomen and is located in the retroperitoneal compartment (Fig. 6). It has a triangular cross section, very similar to the transverse

colon, but, typically, is greater in diameter. The semilunar folds may be slightly thicker than in the transverse colon.

The *hepatic flexure* connects the ascending colon with the transverse colon. It typically has a sharp angle (Fig. 7). The haustral folds at the inner part of colonic flexures and loops can fuse and form complex structures on 2D planar images, which are easily recognized, especially on endoluminal 3D displays [4].

The *transverse colon* extends in an intraperitoneal location from the hepatic to the splenic flexure (Fig. 8). It is the longest portion of the colon and can droop along its mesocolon into the pelvis. Therefore, it is relatively mobile. The transverse colon has a typical triangular cross section formed by the three taeniae. It typically has a distinct haustration.

The *splenic flexure* connects the transverse with the descending colon. It is located below the left diaphragm and is the highest point of the colon. The splenic flexure is often more tortuous than the hepatic flexure and contains, at worst, a series of complex twists (Fig. 9).

The *descending colon* extends into the left abdomen and is located within the retroperitoneal compartment. It is characterized by a straight, tubular shape, with a less triangular to oval cross section (Fig. 10). The haustration is less pronounced than in the proximal colonic segments.

The *sigmoid colon* normally lies within the pelvis and, ideally, has an S-shaped course connecting the descending colon with the rectum (Fig. 11). It is a relatively narrow, mobile, and tortuous segment of the colon with a typically round or oval cross section. The degree of haustration is variable. Due to its intraperitoneal location, there may be a considerable range of movement in the central portion.

The *rectum* is the most distal segment of the colon and has the second largest diameter (Fig. 12) [10]. The upper rectum begins intraperitoneally, but its distal two-thirds are located extraperitoneally. Typically, three distinct semilunar folds are found in the rectum (also referred as Houston's valves or transverse folds). The middle fold, typically the largest one, is more often located at the right side of the rectum [14]. The rectum ends at the anorectal junction (anatomically "linea dentata") and extends to the anal canal. At the anorectal junction, radiating folds are often observed, which are caused by the contraction of the anal sphincter muscles. The anal channel itself cannot be evaluated with CT colonography.

Case 1. Normal Wall Thickness of the Colon

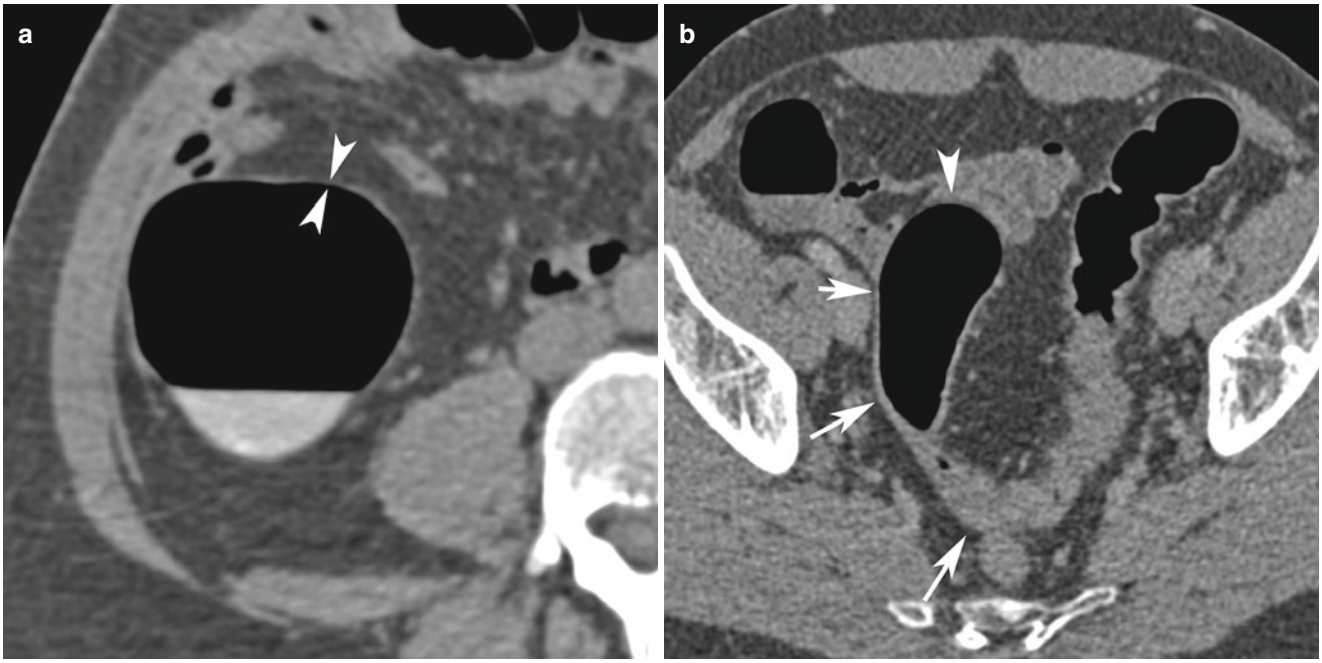

Fig. 1 (**a**) Axial 2D CT image shows the well-distended ascending colon. The colonic wall (*arrowheads*) is barely perceptible. (**b**) Axial 2D CT image shows the partially distended (*arrowheads*) and partially collapsed sigmoid colon. The colonic wall thickness increases gradually (*arrows*) in the collapsed segment

Case 2. CT Morphologic Key Features of the Colon

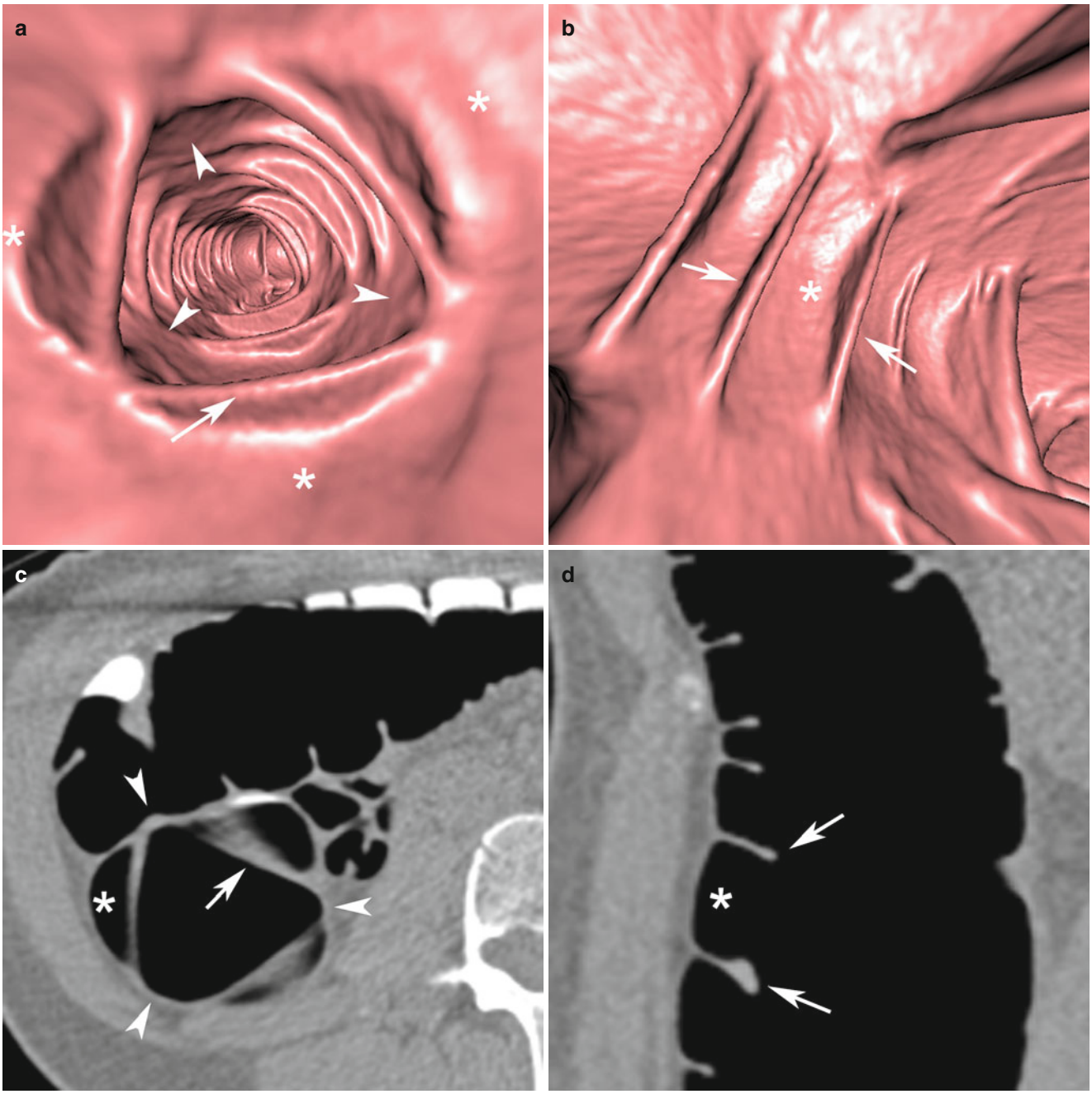

Fig. 2 (**a**) Endoluminal 3D CT image of the ascending colon. Three taeniae are shown as longitudinal bands running along the length of the colon (*arrowheads*). Haustra are located in the spaces between the taeniae (*). (**b**) Endoluminal 3D CT image shows haustra (*) separated by thin semilunar folds (*arrows*). The semilunar folds appear as very thin crescent-shaped structures (*arrows*) (**a**, **b**). (**c**) Axial 2D CT image of the same colonic segment shows corresponding taeniae (*arrowheads*), semilunar folds (*arrow*) as thin soft tissue dense structures, and the haustra (*). Note the triangular cross section of the ascending colon. (**d**) Coronal 2D CT image showing haustra (*) separated by thin semilunar folds (*arrows*)

Case 3. Six Segments of a Normal Colon

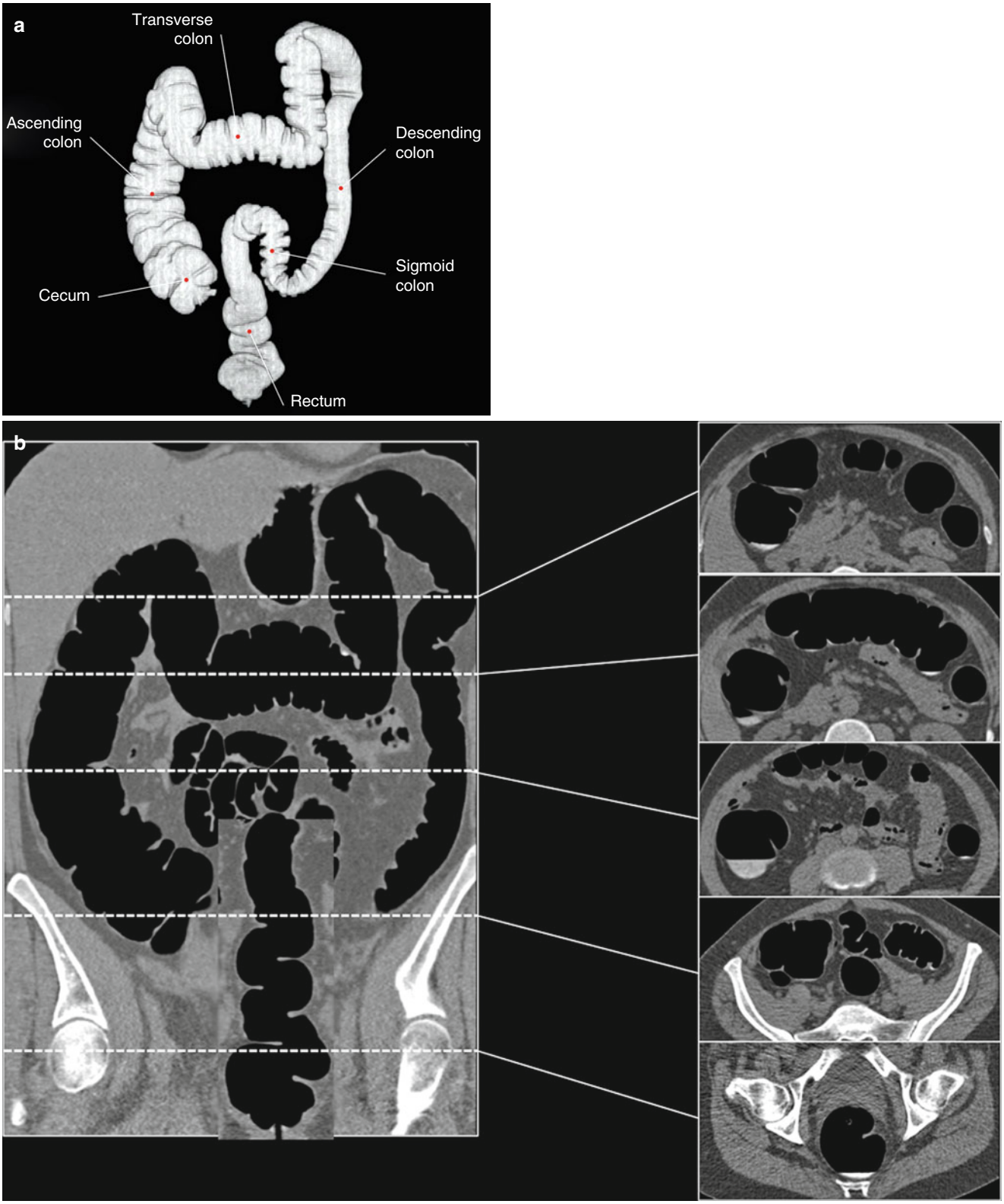

Fig. 3 (**a**) Global surface-rendered 3D view shows the cecum, ascending colon, transverse colon, descending colon, and the rectum. All segments are of normal location, length, and diameter. (**b**) Coronal 2D CPR illustrates the course of the colon and rectum (inlay) (*left*). Corresponding axial 2D CT images show the location of the colonic segments (*right*)

Case 4. Cecum: Triradiate Fold and Appendiceal Orifice

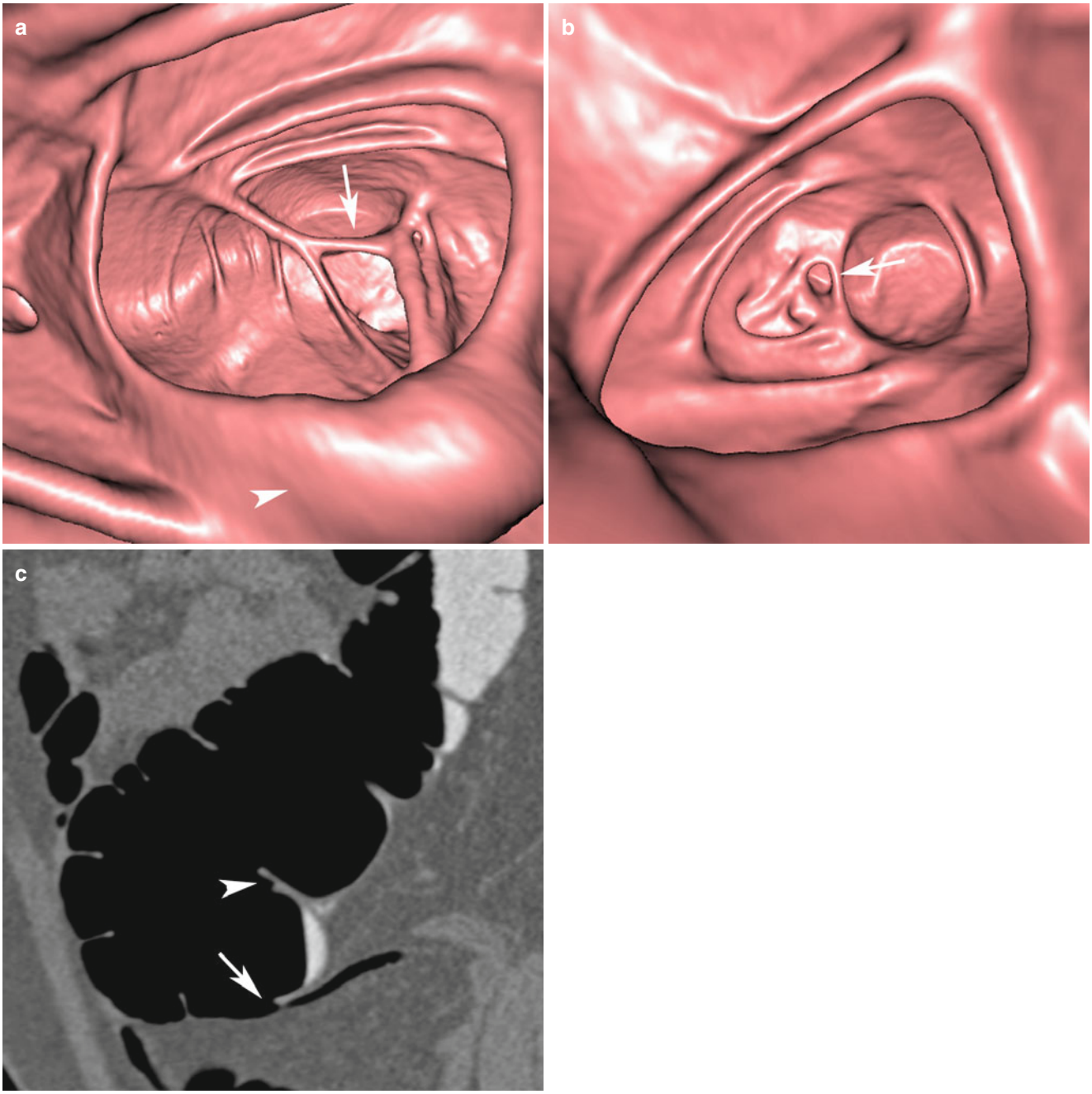

Fig. 4 (**a**) Retrograde endoluminal 3D CT image of the cecum, showing the three colonic taeniae converging and forming the triradiate fold (*arrow*). Note the papillary ileocecal valve (*arrowhead*). (**b**) Retrograde endoluminal 3D CT image of the cecum in another patient, showing the appendiceal orifice at the area of the triradiate fold (*arrow*), appearing as a small, well-circumscribed, round depression. (**c**) Coronal 2D image showing the blind end of the cecum in the right iliac fossa. Note the labial ileocecal valve (*arrowhead*) on the medial aspect of the cecum and the appendiceal orifice (*arrow*) at the cecal base. The appendix is filled with air

Case 5. Cecum: Normal Labial Ileocecal Valve

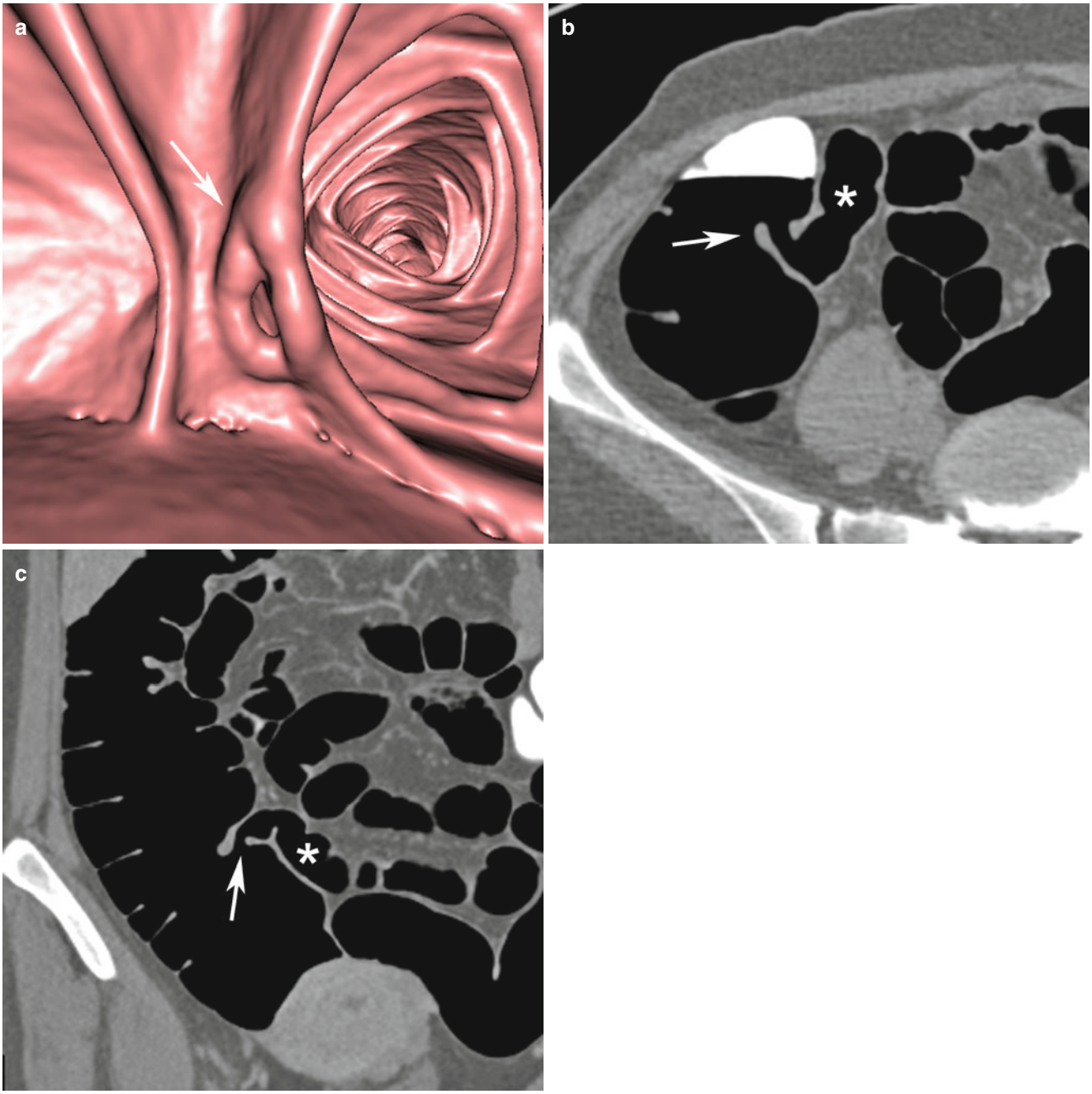

Fig. 5 (**a**) Antegrade endoluminal 3D CT view from the cecum into the ascending colon, showing the ileocecal valve (*arrow*) with an upper and lower lip and, in between, the opened orifice. (**b**, **c**) Axial and coronal 2D CT image showing the blind-ending cecum in the right iliac fossa. The ileocecal valve is located on the medial side of the cecum and shows the open orifice with an upper and a lower lip (*arrow*). Note the connection of the terminal ileum (*) to the valve

Case 6. Ascending Colon

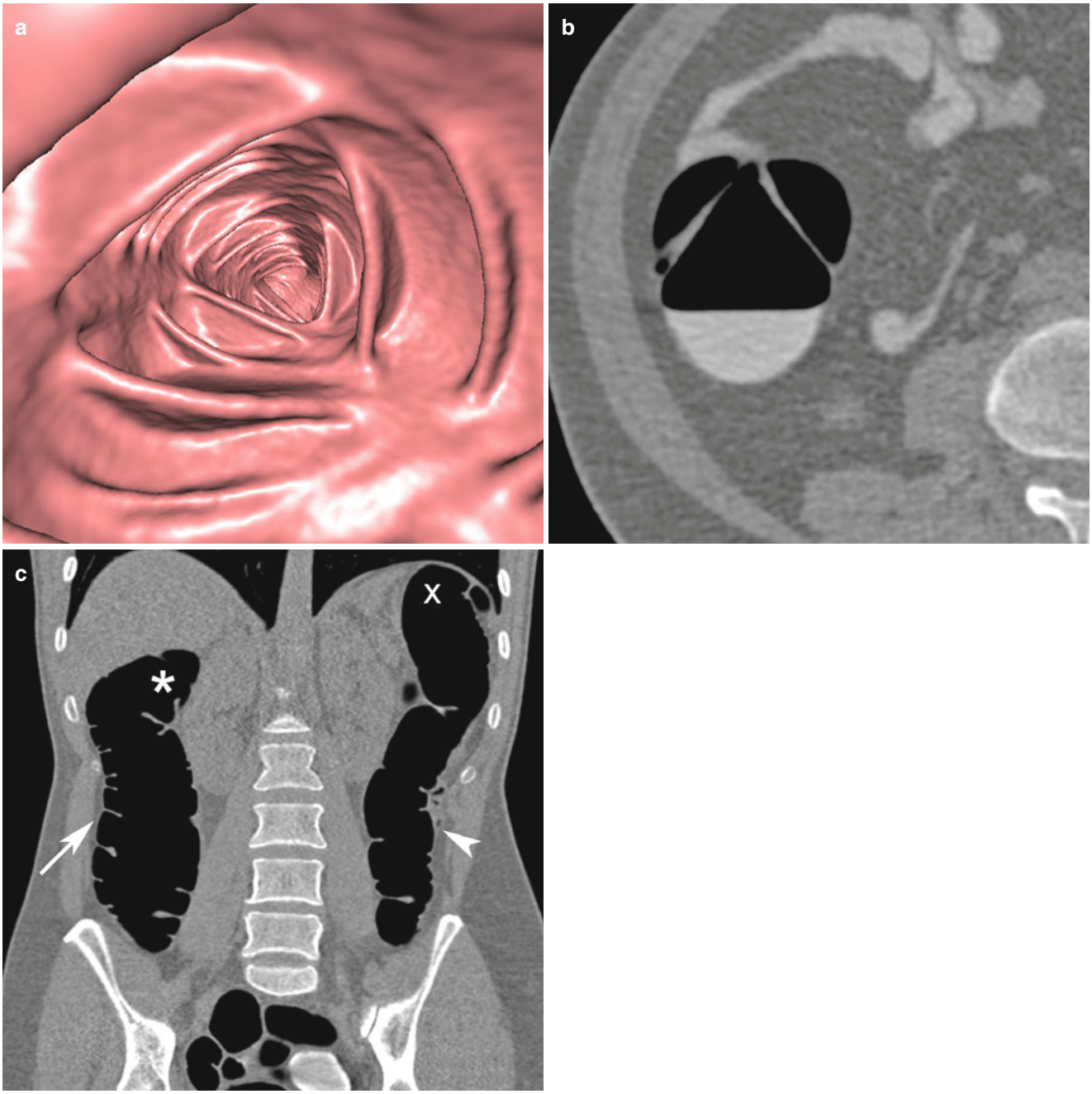

Fig. 6 (**a**) Antegrade endoluminal 3D CT view and (**b**) axial 2D CT image of the ascending colon, showing a triangular cross section and distinct haustration. (**c**) Coronal 2D CT image showing the ascending colon (*arrow*) extending retroperitoneally into the right abdomen. Note the right (*) and left (X) flexure and the descending colon (*arrowhead*)

Case 7. Right Flexure

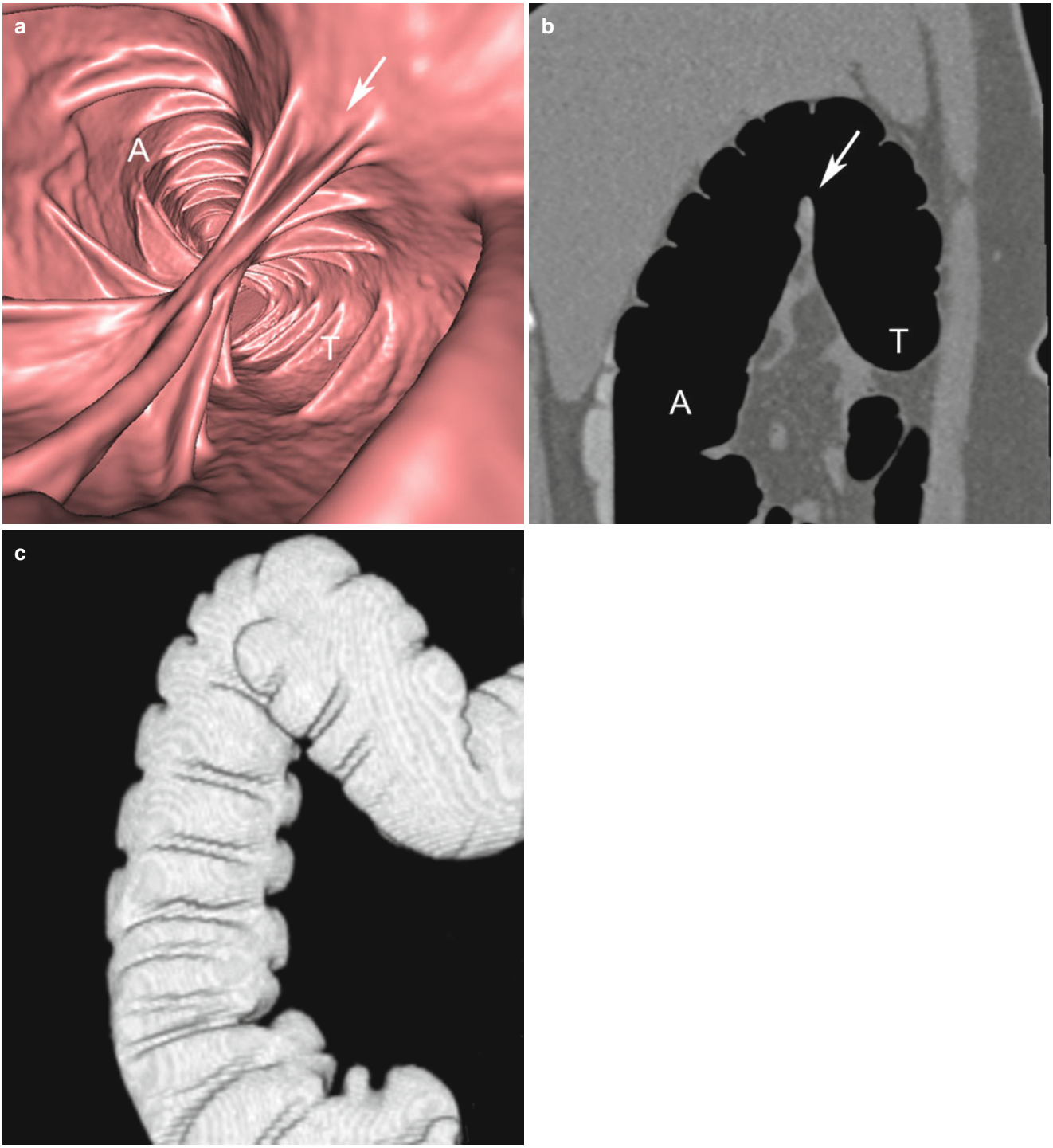

Fig. 7 (**a**) Endoluminal 3D CT view and (**b**) sagittal 2D image showing the right flexure (*arrow*) connecting the ascending (*A*) with the transverse (*T*) colon and forming a relatively sharp angle. (**b**) Sagittal 2D CT image showing the thickened fold pattern at the inner part of the right flexure (*arrow*), which is easily realized on endoluminal 3D views. *A* ascending colon, *T* transverse colon. (**c**) Global surface-rendered 3D view shows the course of the right flexure

Case 8. Transverse Colon

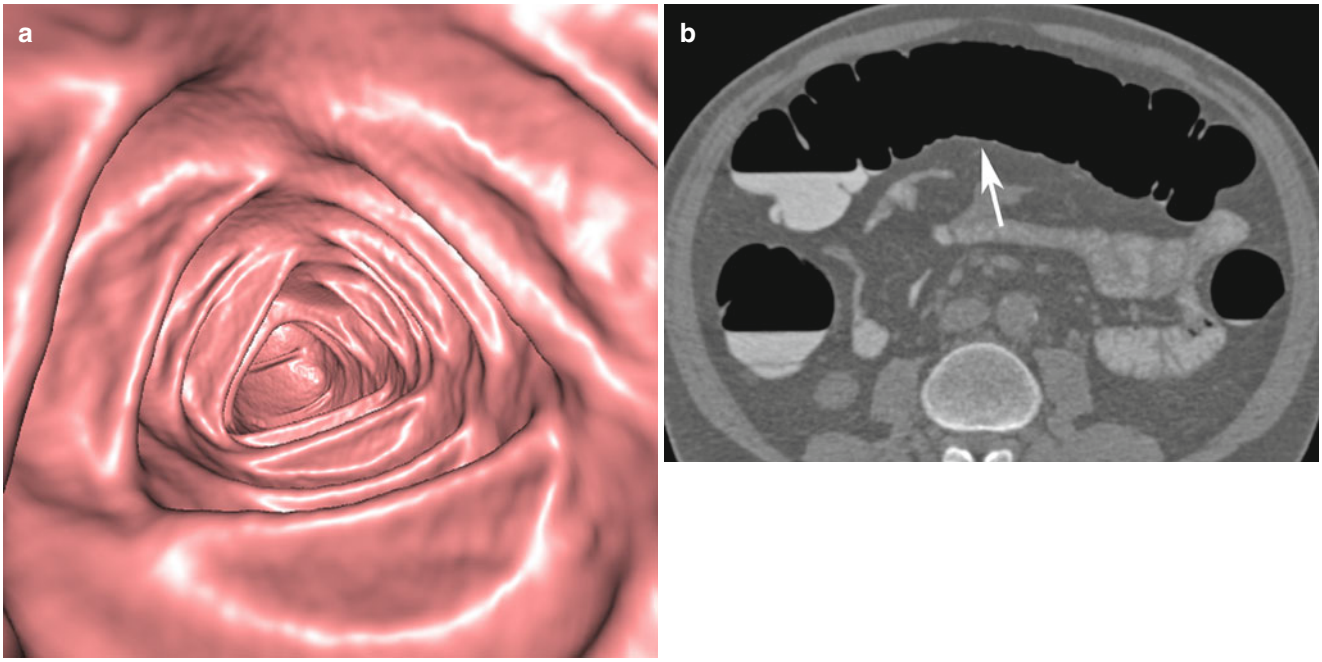

Fig. 8 (**a**) Endoluminal 3D CT image of the transverse colon with a typical triangular lumen formed by the three taeniae and with a distinct haustration. The diameter is slightly smaller than in the ascending colon. (**b**) Axial 2D CT image showing the course of the transverse colon (*arrow*) connecting the ascending colon on the *right side* and the descending colon on the *left side*

Case 9. Left Flexure

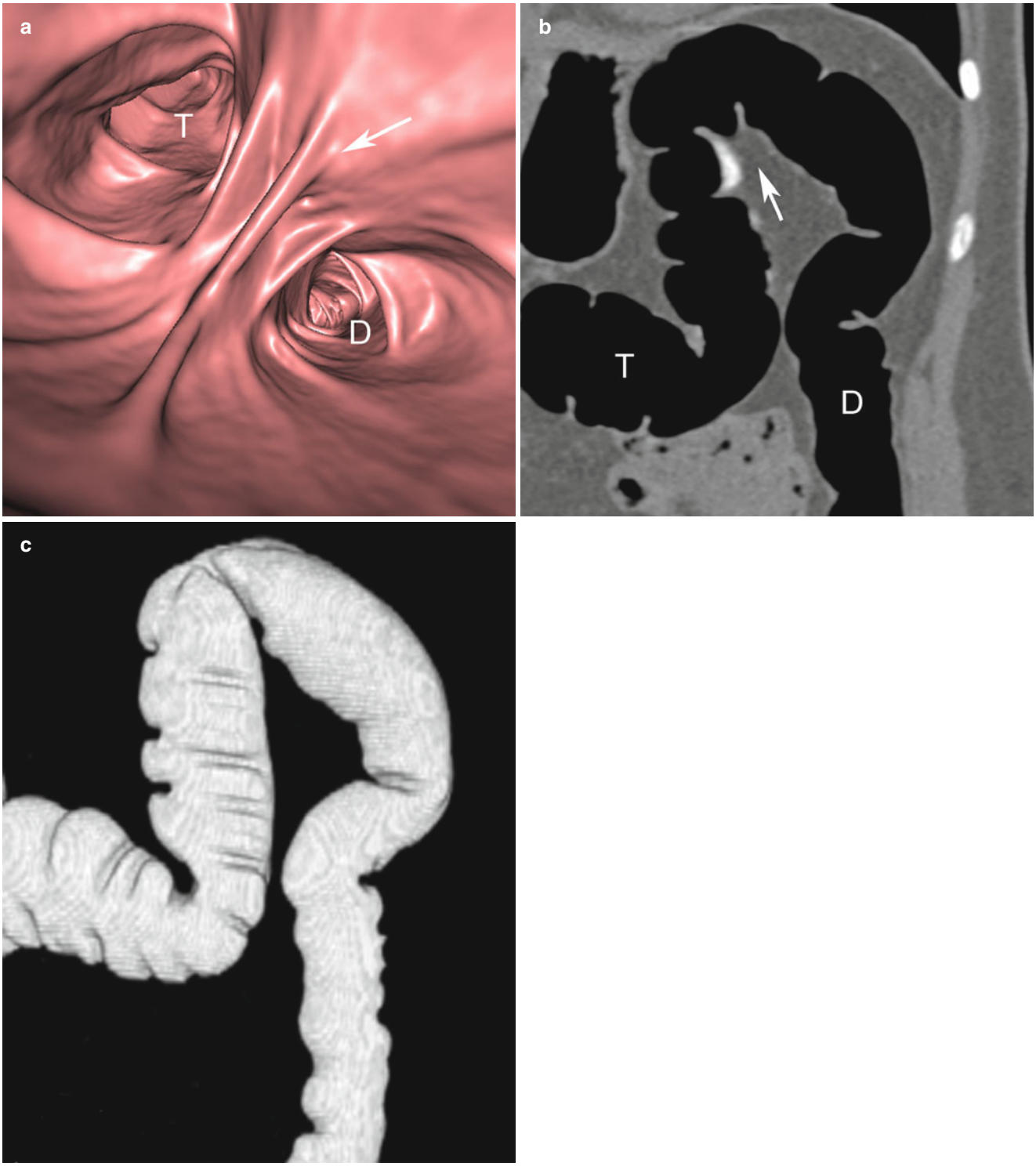

Fig. 9 (**a**) Endoluminal 3D CT view and (**b**) sagittal 2D image showing the left flexure (*arrow*) connecting the transverse (*T*) with the descending (*D*) colon. (**b**) Sagittal 2D CT image showing the complex fold pattern at the inner part of the left flexure (*arrow*), being more tortuous than the hepatic flexure. *T* transverse colon, *D* descending colon. (**c**) Global surface-rendered 3D view shows the course of the left flexure

Case 10. Descending Colon

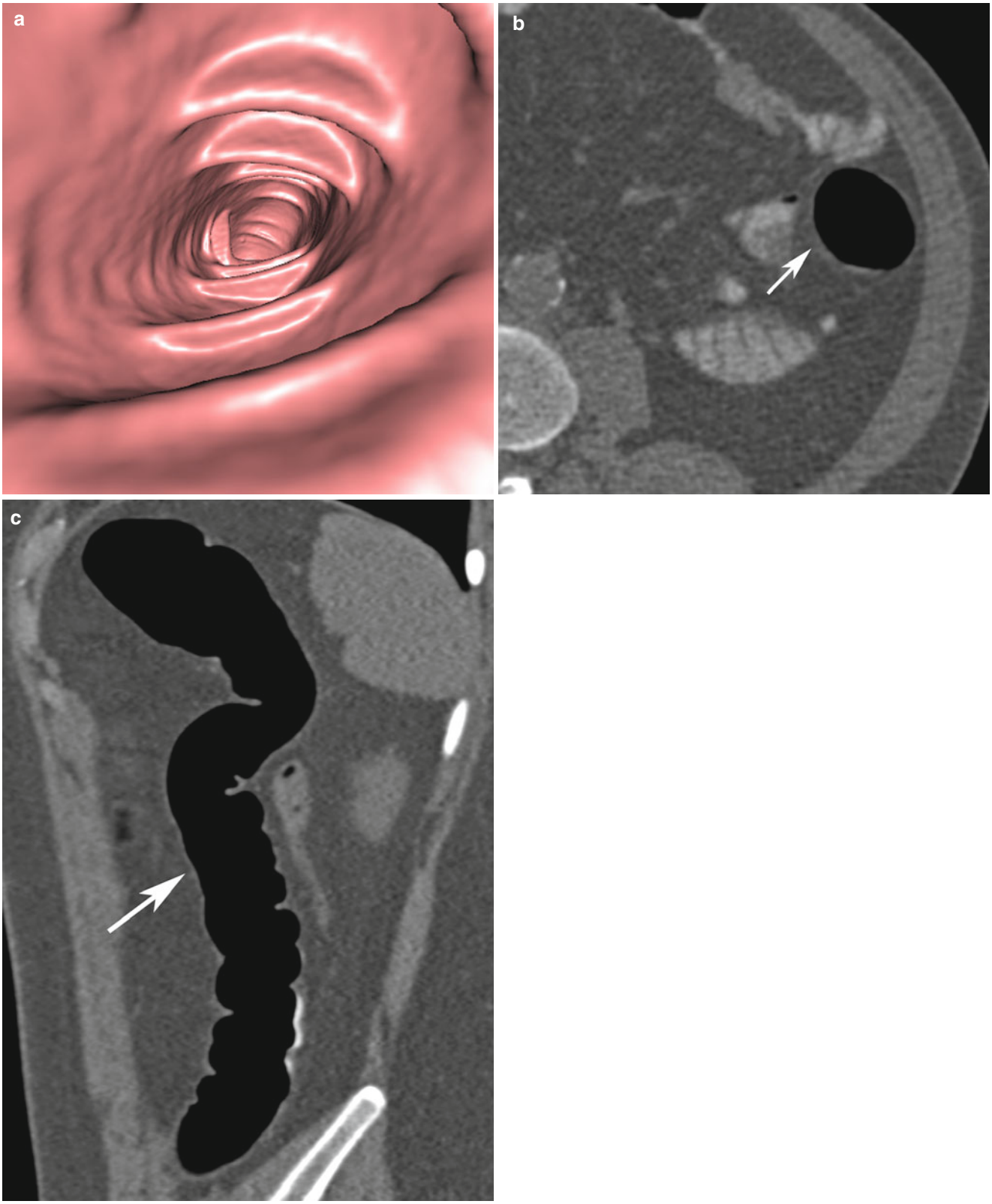

Fig. 10 (**a**) Antegrade endoluminal 3D CT view and axial 2D CT image of the descending colon, showing a round lumen compared to the triangular lumen in the transverse colon (see Fig. 8a). Note that the diameter is smaller in comparison to the upper colonic segments. (**b**) Axial 2D CT image showing the descending colon located in the left abdomen with a round cross section of (*arrow*). (**c**) Sagittal 2D view showing the straight and tubular shape of the descending colon (*arrow*)

Case 11. Sigmoid Colon

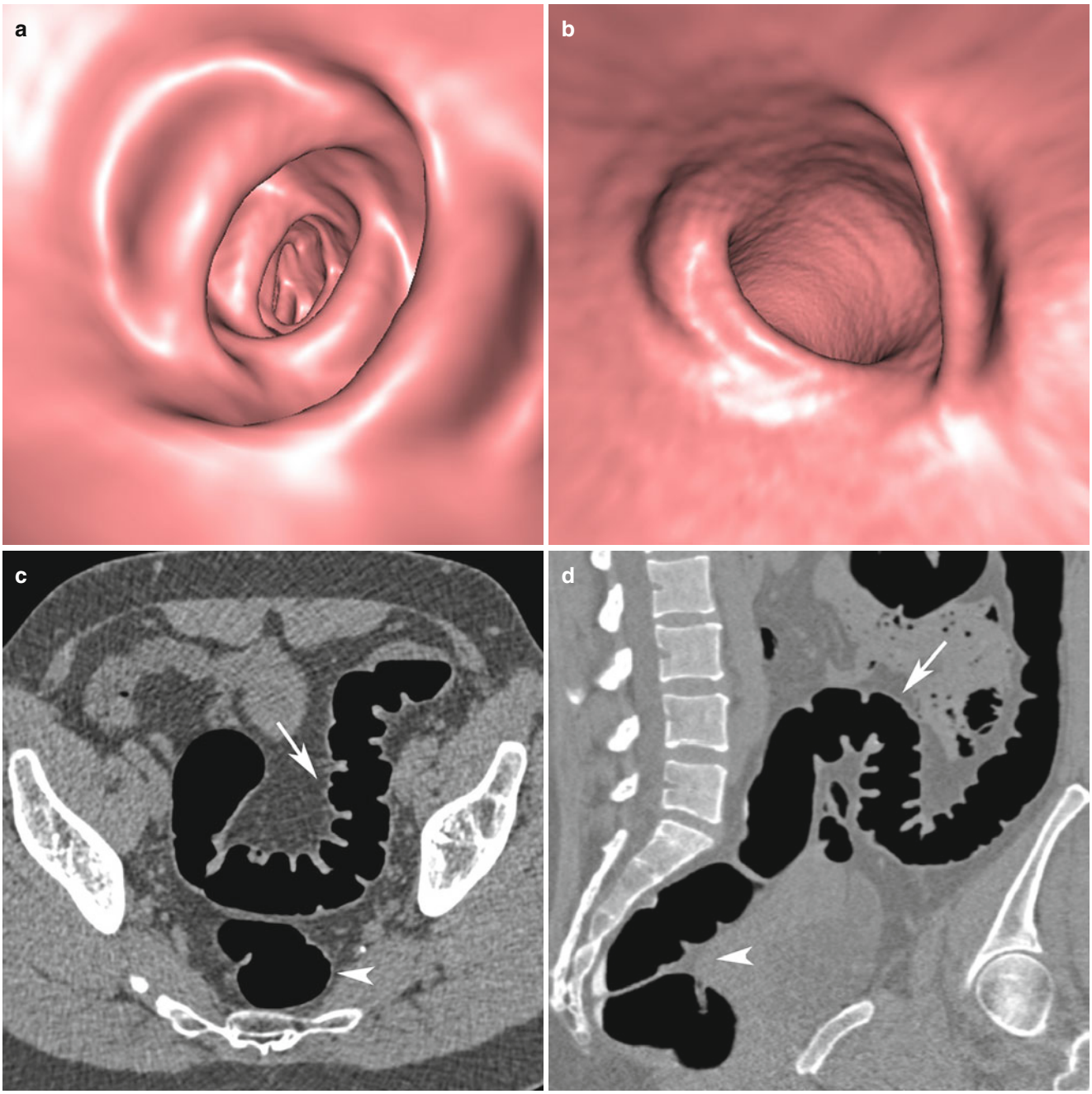

Fig. 11 Sigmoid colon. (**a**, **b**) Endoluminal 3D views from two different patients show a relatively narrow lumen with a typically round or oval cross section. The degree of haustration is variable and can be pronounced (**a**) or low (**b**). (**c**) Axial unenhanced prone 2D CT image and (**d**) sagittal 2D CPR show the typical S-shaped course of the sigmoid colon (*arrow*), connecting the descending colon with the rectum (*arrowhead*)

Case 12. Rectum

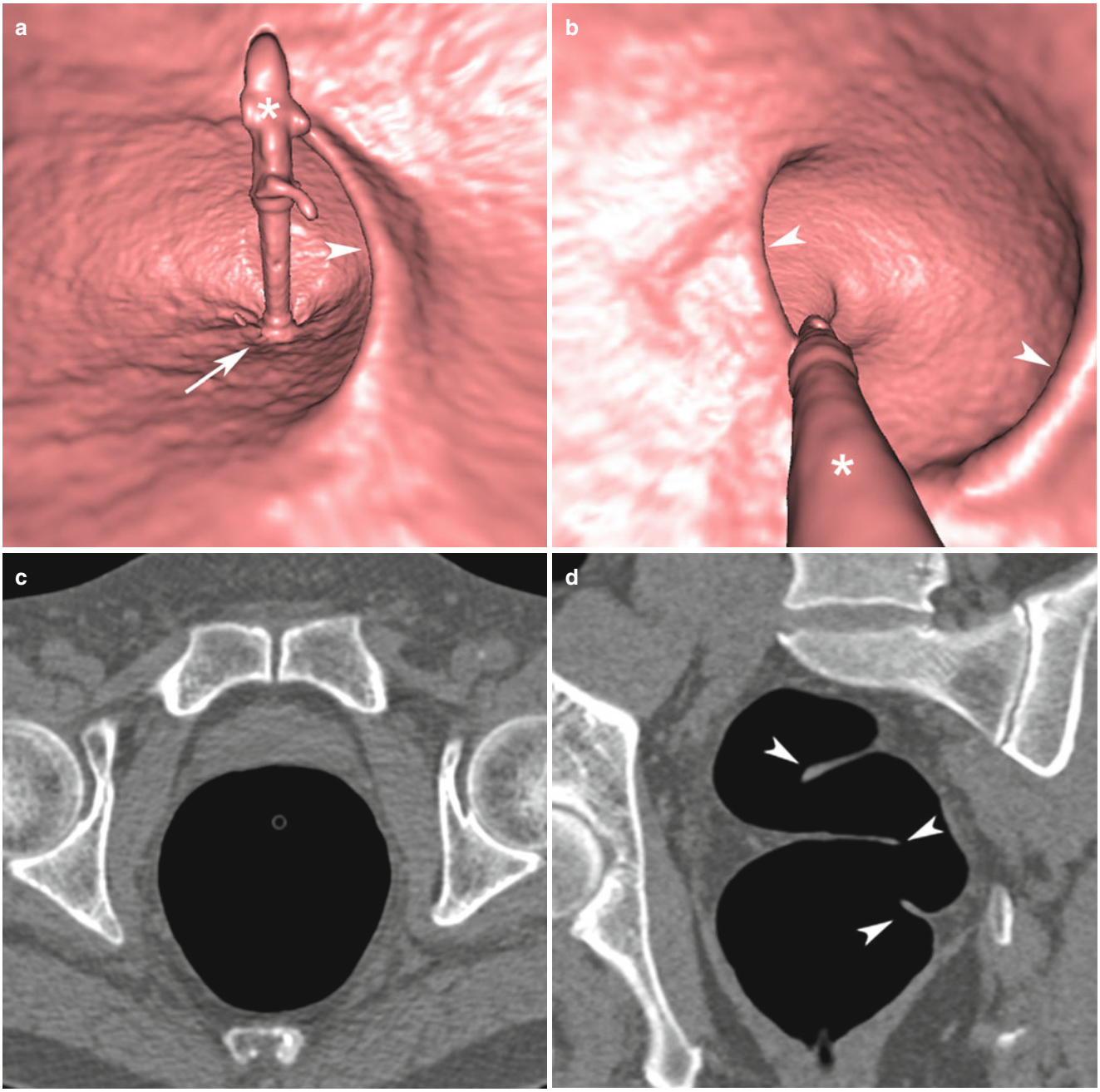

Fig. 12 (**a**) Antegrade endoluminal 3D view shows small radiating folds (*arrow*) at the anorectal junction caused by contraction of the anal sphincter muscles. Distal transverse rectal fold (*arrowhead*) and rectal tube (*). (**b**) Retrograde endoluminal 3D view showing two transverse rectal folds (*arrowheads*) and the rectal tube (*). (**c**) Axial 2D CT image shows a well-distended rectum with a large diameter will provide ane fig with 3 arrowheads and without the arrow. (**d**) Coronal 2D CT image shows three distinct semilunar rectal folds (*arrowheads*) that were found in the rectum (Houston's valves)

References

1. Fenlon HM, Clarke PD, Ferrucci JT (1998) Virtual colonoscopy: imaging features with colonoscopic correlation. AJR Am J Roentgenol 170(5):1303–1309
2. Macari M, Megibow AJ (2001) Pitfalls of using three-dimensional CT colonography with two-dimensional imaging correlation. AJR Am J Roentgenol 176(1):137–143
3. Silva AC, Wellnitz CV, Hara AK (2006) Three-dimensional virtual dissection at CT colonography: unraveling the colon to search for lesions. Radiographics 26(6):1669–1686
4. Mang T, Maier A, Plank C, Mueller-Mang C, Herold C, Schima W (2007) Pitfalls in multi-detector row CT colonography: a systematic approach. Radiographics 27(2):431–454
5. Neri E, Halligan S, Hellström M (2012) ESGAR CT Colonography Working Group. Eur Radiol. Sep 15. [Epub ahead of print] PMID: 22983280
6. Wiesner W, Mortele KJ, Ji H, Ros PR (2002) Normal colonic wall thickness at CT and its relation to colonic distension. J Comput Assist Tomogr 26(1):102–106
7. Mang T, Schima W (2009) CT-Kolonographie, 1st ed. Georg Thieme Verlag, Stuttgart
8. Horton KM, Corl FM, Fishman EK (2000) CT evaluation of the colon: inflammatory disease. Radiographics 20(2):399–418
9. Zalis ME, Barish MA, Choi JR et al (2005) CT colonography reporting and data system: a consensus proposal. Radiology 236(1):3–9
10. Khashab MA, Pickhardt PJ, Kim DH, Rex DK (2009) Colorectal anatomy in adults at computed tomography colonography: normal distribution and the effect of age, sex, and body mass index. Endoscopy 41(8):674–678
11. Silva AC, Beaty SD, Hara AK et al (2007) Spectrum of normal and abnormal CT appearances of the ileocecal valve and cecum with endoscopic and surgical correlation. Radiographics 27(4):1039–1054
12. Iafrate F, Rengo M, Ferrari R, Paolantonio P, Celestre M, Laghi A (2007) Spectrum of normal findings, anatomic variants and pathology of ileocecal valve: CT colonography appearances and endoscopic correlation. Abdom Imaging 32(5):589–595
13. Regge D, Gallo TM, Nieddu G et al (2005) Ileocecal valve imaging on computed tomographic colonography. Abdom Imaging 30(1):20–25
14. Silva AC, Vens EA, Hara AK, Fletcher JG, Fidler JL, Johnson CD (2006) Evaluation of benign and malignant rectal lesions with CT colonography and endoscopic correlation. Radiographics 26(4): 1085–1099